HHS Public Access

Author manuscript

Neuroimage. Author manuscript; available in PMC 2018 December 06.

Published in final edited form as:

Neuroimage. 2014 January 01; 84: 868–875. doi:10.1016/j.neuroimage.2013.09.021.

Neuroinflammation in healthy aging: A PET study using a novel Translocator Protein 18 kDa (TSPO) radioligand, [18F]-FEPPA

I. Suridjan[a], **P.M. Rusjan**[a], **A.N. Voineskos**[a,b], **T. Selvanathan**[a], **E. Setiawan**[a], **A.P. Strafella**[a,c], **A.A. Wilson**[a,b], **J.H. Meyer**[a,b], **S. Houle**[a], and **R. Mizrahi**[a,b,*]

[a]Research Imaging Centre, Centre for Addiction and Mental Health, 250 College Street, M5T 1R8, Toronto, Ontario, Canada

[b]Department of Psychiatry, University of Toronto, 27 King's College Circle, M5S 1A1, Ontario, Canada

[c]Division of Brain Imaging & Behavior-Systems Neuroscience, Toronto Western Research Institute, UHN, 399 Bathurst Street, M5T 2S8, Ontario, Canada

Abstract

One of the cellular markers of neuroinflammation is increased microglia activation, characterized by overexpression of mitochondrial 18 kDa Translocator Protein (TSPO). TSPO expression can be quantified in-vivo using the positron emission tomography (PET) radioligand [^{18}F]-FEPPA. This study examined microglial activation as measured with [^{18}F]-FEPPA PET across the adult lifespan in a group of healthy volunteers. We performed genotyping for the rs6971 TS.PO gene polymorphism to control for the known variability in binding affinity. Thirty-three healthy volunteers (age range: 19–82 years; 22 high affinity binders (HAB), 11 mixed affinity binders (MAB)) underwent [^{18}F]-FEPPA PET scans, acquired on the High Resolution Research Tomograph (HRRT) and analyzed using a 2-tissue compartment model. Regression analyses were performed to examine the effect of age adjusting for genetic status on [^{18}F]-FEPPA total distribution volumes (V_T) in the hippocampus, temporal, and prefrontal cortex. We found no significant effect of age on [^{18}F]-FEPPA V_T ($F(1,30) = 0.918$; $p = 0.346$), and a significant effect of genetic polymorphism ($F(1,30) = 8.767$; $p = 0.006$). This is the first in-vivo study to evaluate age-related changes in TSPO binding, using the new generation TSPO radioligands. Increased neuroinflammation, as measured with [^{18}F]-FEPPA PET was not associated with normal aging, suggesting that healthy elderly individuals may serve as useful benchmark against patients with neurodegenerative disorders where neuroinflammation may be present.

Keywords

Neuroinflammation; PET imaging; Microglia activation; TSPO; Healthy aging; [^{18}F]-FEPPA

*Corresponding author at: Research Imaging Centre, Centre for Addiction and Mental Health, 250 College Street, M5T 1R8, Toronto, Ontario, Canada. Fax: +1 416 979 4656. romina.mizrahi@camhpet.ca (R. Mizrahi).

Financial disclosure

Authors have no financial interests related to this work.

Conflict of interest

Authors have no conflict of interest with the present work.

Introduction

Neuroinflammation is believed to be involved in several neurological disorders, especially those in which age is a risk factor (Block and Hong, 2005). While inflammatory processes are necessary and important mechanisms of the brain to remove debris and foreign invaders, chronic inflammatory reactions may damage healthy tissue and can be neurotoxic. The microglia cells are the resident macrophages of the brain and thought to have an immunosurveillence role in the central nervous system (CNS). Microglia become activated in response to various neuronal insults, and this activation is considered as one of the cellular features of neuroinflammation (Gehrmann et al., 1995). Increased density of activated microglia has been reported in several age-related neurodegenerative diseases, such as in patients with Mild Cognitive Impairment (MCI) (Wiley et al., 2009), Alzheimer's disease (AD) (Cagnin et al., 2001; Edison et al., 2008; Yasuno et al., 2008), frontotemporal dementia (Cagnin et al., 2004), ischemic stroke (Gerhard et al., 2000; Pappata et al., 2000), and Parkinson's disease (Gerhard et al., 2006; Ouchi et al., 2005). Any changes in microglia function that occur during normal aging may adversely affect neuronal integrity and function. In fact, age related decline in cognitive performance is associated with altered levels of pro-inflammatory cytokines, a process that is possibly mediated by changes in microglia function (Lekander et al., 2011).

Aged microglia undergo changes in morphology, function, and dynamic behavior (Damani et al., 2011; Njie et al., 2012; Peters et al., 1991; Vaughan and Peters, 1974). In a resting state, aged microglia display significantly smaller and less branched dendritic arbors, more inclusions within their cytoplasm, and higher expression of surface proteins associated with activation (Damani et al., 2011; Peters et al., 1991; Sheffield and Berman, 1998). They show slower response and less ramified morphology following injury, suggesting a possible age-dependent deregulation of CNS immune response (Damani et al., 2011). Non-human primates with impaired cognitive function present significantly higher density of activated microglia in the white matter of cingulate gyrus and the corpus callosum (Sloane et al., 1999). Further, microglia derived from aging mice exhibit increased mRNA expression of pro-inflammatory cytokines (IL-1β, IL-6, and TNF-α) following inflammatory lipopolysaccharide stimulation, suggesting that an exaggerated inflammatory response occurs in healthy aging (Godbout and Johnson, 2006; Henry et al., 2009; Njie et al., 2012; Sierra et al., 2007). Consistent with these animal studies, several post-mortem human studies have also indicated a significant age-related alteration in microglia morphology and function, as well as age-associated increases in the total number of activated microglia (DiPatre and Gelman, 1997; Miller and Streit, 2007; Sheffield and Berman, 1998; Sheng et al., 1998). Collectively, these studies suggest an active role of microglia in normal brain aging.

Regional selective gray matter volume loss is linked to a cognitive decline (Hutton et al., 2009; Jack et al., 1997; Tisserand et al., 2004). In a seminal longitudinal study of patients with mild AD, an association between cortical atrophy and neuroinflammation was reported; showing that a greater number of activated microglia at baseline was a significant predictor of greater volume loss 12 and 24 months later (Cagnin et al., 2001).

The Translocator Protein 18 kDa (TSPO) is a hetero-oliomeric complex protein located in the outer mitochondrial membrane of microglia (Chen and Guilarte, 2008). Increased TSPO expression is recognized as a reliable biomarker of activated microglia both in vitro and in vivo (Venneti et al., 2009). Studies investigating the relationship between aging and TSPO overexpression are sparse and the results from these studies are mixed. In-vitro study using human platelet cells showed a non-significant difference in TSPO density between young and older subjects (Marazziti et al., 1994). However, a radioligand binding assay study using the classical TSPO radioligand [^{3}H]-PK11195 in an animal model of aging showed an age-related increase in TSPO binding in the cerebral cortex and hippocampus (Nomura et al., 1996).

The first positron emission tomography (PET) study examining the relationship between age and TSPO binding in humans was carried out using [^{11}C]-PK11195. This study did not observe significant associations between age and regional [^{11}C]-PK11195 binding in most regions of the brain except in the thalamus, where an age-dependent increase was found (Cagnin et al., 2001). However, as a TSPO radioligand, [^{11}C] PK11195 has important limitations including a relatively high noise to signal ratio due to high nonspecific binding, low brain penetration, and high plasma protein binding (Chauveau et al., 2008).

Here, we present the first study evaluating the effect of age on neuroinflammation using a second-generation TSPO radioligand, [^{18}F]-FEPPA. [^{18}F]-FEPPA has a high affinity for TSPO, an appropriate metabolic profile, with high brain penetration and good pharmacokinetics (Wilson et al., 2008). Previous PET (Fujita et al., 2008; Kreisl et al., 2010) and in-vitro studies (Owen et al., 2010, 2011) with second generation TSPO radioligands revealed significant inter-subject variability due to differences in binding affinity. Three types of binders were reported: high affinity binders (HAB), low-affinity binders (LAB), and mixed-affinity binders (MAB) (Owen et al., 2010, 2011). A single polymorphism (rs6971) located in the exon 4 of the TSPO gene results in a nonconservative amino-acid substitution from alanine to threonine (Ala147Thr) in the TSPO protein. This polymorphism predicts [^{11}C]-PBR28 and [^{18}F]-FEPPA binding affinity class in the brain (Kreisl et al., 2013; Mizrahi et al., 2012; Owen et al., 2012).

The influence of rs6971 polymorphism has never been accounted for in previous PET studies examining age and neuroinflammation (Cagnin et al., 2001; Kumar et al., 2012; Schuitemaker et al., 2010). We hypothesized that age-related differences in [^{18}F]-FEPPA binding would be observed in the hippocampus, prefrontal, and temporal cortex, after controlling for the contribution of genetic variation on binding affinity. These were brain regions showing higher TSPO expression in patients with age-related neurological disorders such as AD and MCI (Cagnin et al., 2001; Okello et al., 2009; Wiley et al., 2009). Further, given that age is strongly associated with volume loss, particularly in the prefrontal and temporal cortex (Jernigan et al., 2001; Raz et al., 1997; Salat et al., 1999, 2001; Tisserand et al., 2002), our exploratory aim was to investigate whether brain areas susceptible to age-related volume loss would be the same areas showing age-related increase in [^{18}F]-FEPPA uptake.

Materials and methods

Participants

Thirty-three healthy individuals were screened and ruled out of any present or past axis I disorders using the Structured Clinical Interview for DSM-IV by the study psychiatrist (RM). All participants were also screened to rule out current medical illness based on history, physical examination, and urinalysis (including urine toxicology). Participants with history of cardiovascular events, stroke or other neurological diseases were excluded. All participants underwent one [^{18}F]-FEPPA PET scan and one magnetic resonance imaging (MRI) scan. For the MRI scan, the T1-weighted MRI was acquired to use for image co-registration with the PET image and evaluation of cortical volumes (described below). The PD-weighted MRI was visually inspected for evidence of focal and vascular lesions including the presence of lacunar infarcts and white matter hyperintensities.

Participants completed the Mini Mental State Examination test (MMSE) to assess global cognitive mental status. Each subject underwent one [^{18}F]-FEPPA PET scan and one magnetic resonance imaging (MRI) scan. Blood samples were collected for genotyping of TSPO rs6971 polymorphism and to obtain arterial input function for the kinetic analysis of [^{18}F]-FEPPA (described in detail below).

All participants provided written informed consent after all procedures were fully explained. The study and recruitment procedures were approved by the Research Ethics Board for human subjects at the Centre for Addiction and Mental Health, University of Toronto.

[^{18}F]-FEPPA synthesis

The synthesis of [^{18}F]-FEPPA has been described elsewhere (Wilson et al., 2008). It can be reliably and quickly labeled with [^{18}F] by nucleophilic displacement of a tosylate leaving group in a fast one-step reaction. Purification and formulation yield a sterile and pyrogen-free product (Wilson et al., 2008).

Image acquisition and analysis

A dose of 185 ± 20 MBq (5 ± 0.5 mCi) of intravenous [^{18}F]-FEPPA was administered as a bolus for the PET scan. An automatic blood sampling system (ABSS, Model #PBS-101 from Veenstra Instruments, Netherland) was used to measure arterial blood radioactivity continuously at a rate of 2.5 ml/min for the first 22.5 min. Manual arterial blood samples were obtained at 2.5, 7, 12, 15, 30, 45, 60, 90, and 120 min. The manual samples were used to determine the radioactivity in whole blood and plasma and the plasma metabolite composition. The ratio of radioactivity in whole blood to radioactivity in plasma was fitted by a bi-exponential and used as a correction factor to be applied to the blood radioactivity time activity curve obtained from automatic sampling in order to generate the plasma radioactivity curve. The fraction of parent radioligand in plasma was determined by HPLC analysis and was fitted with a Hill function. The blood curve was divided by the bi exponential fitting the ratio blood to plasma, multiplied by the hill function and corrected for delay and dispersion to generate a parent compound in plasma curve to use as input function for the kinetic analysis (for further details, please see Rusjan et al., 2011).

The scan duration was 125 min following the injection of [^{18}F]-FEPPA. The images were reconstructed into 34 time frames. Frames were acquired as follows: 1 frame of variable length until the radioactivity appears in the field of view (FOV), 5 frames of 30 s, 1 frame of 45 s, 2 frames of 60 s, 1 frame of 90 s, 1 frame of 120 s, 1 frame of 210 s, and 22 frames of 300 s. The PET images were obtained using a 3D High Resolution Research Tomography (HRRT) (CS/Siemens, Knoxville, TN, USA), which measures radioactivity in 207 slices with an inter-slice distance of 1.22 mm. All PET images were corrected for attenuation using a single photon point source, ^{137}Cs ($T_{0.5}$ = 30.2 years, Eγ = 662 keV) and were reconstructed by filtered back projection algorithm using a HANN filter at Nyquist cutoff frequency. The reconstructed image has 256 × 256 × 207 cubic voxels measuring 1.22 × 1.22 × 1.22 mm^3 and the resulting reconstructed resolution is close to isotropic 4.4 mm, full width at half maximum in plane and 4.5 mm full width at half maximum axially, averaged over measurements from the center of the transaxial FOV to 10 cm off-center in 1.0 cm increments.

Region of interest (ROI)-based analysis

For the anatomical delineation of region of interest (ROIs), a brain MRI was used for each subject. On twenty-six of our subjects, T1 weighted images were acquired with a General Electric (Milwaukee, WI, USA) Signa 1.5 T magnetic resonance image scanner (slice thickness = 1.5 mm, repetition time (TR) = 12, echo time (TE) = Min full, flip angle = 20°, number of excitations (NEX) = 1, acquisition matrix = 256 × 256, and Field of View = 20 cm). On seven of our subjects, the T1 weighted images were acquired with a 3-Telsa General Electric MR750 scanner (slice thickness = 0.9 mm, TR = 8.2 ms, TE = Min full, flip angle = 8°, NEX = 1, acquisition matrix = 256 × 228, and Field of View = 28 cm).

ROIs were automatically generated using our in-house imaging pipeline, ROMI, which has been previously described in (Rusjan et al., 2006). Four ROIs were included in the analysis: prefrontal cortex, dorsolateral prefrontal cortex (DLPFC), temporal cortex, and hippocampus (Maldjian et al., 2003; Rajkowska and Goldman-Rakic, 1995a,b). Briefly, ROMI fits a standard template of ROIs to an individual high-resolution T1 MRI scan based on the probability of gray matter, white matter, and CSF. The individual MR images are then co-registered to each summed [^{18}F]-FEPPA PET image using the normalized mutual information algorithm (Studholme et al., 1997) and the resulting rigid body transformation was applied to the ROIs, to mask the PET image and to generate the time activity curve (TAC) for each ROI.

To address the potential issues of bias from the volume loss in the older subjects, time activity data for all subjects was corrected for the effect of partial volume error (PVE) using the Mueller-Gartner partial volume error correction algorithm (Muller-Gartner et al., 1992) as implemented in Bencherif et al. (2004).

The kinetics of [^{18}F]-FEPPA can be described with a two tissue compartment model (2-TCM) using [^{18}F]-FEPPA radioactivity in arterial plasma as an input function (as described in Rusjan et al., 2011) and a 5% vascular contribution. Our outcome measure is the Total distribution volume (V_T), which is a ratio at equilibrium of the radioligand concentration in tissue to that in plasma (i.e. specific binding and non-displaceable uptake, which includes

non-specifically bound and free radioligand in tissue). The V_T for 2-TCM can be expressed in terms of kinetic rate parameters as: $V_T = K_1 / k_2 (1 + k_3 / k_4)$ where K_1 and k_2 are influx and efflux rates for radiotracer passage across the blood–brain barrier and k_3 and k_4 describe the radioligand transfer between the free and non-specific compartment and the specific binding compartment.

Cortical volumes

ROI-based volumetric analysis was obtained after all ROIs were automatically delineated in each individual's MRI, regional gray matter volumes were obtained by multiplying the number of gray matter voxels in each ROIs to the volume of the voxel in the T1-MRI. The regional gray matter volumes were divided by the subjects' total intracranial volume (ICV), which is strongly related to premorbid absolute brain volume and does not change with age. Thus, when regional volumes are normalized by the ICV, the resulting measurement provides an index of atrophy of the region and corrects for the potential confounding factors of head size effects across age or sex between subject groups. Data are presented as a ratio of each region relative to the ICV, and termed as the Volume of Interest ratio (VOI ratio). We delineated four VOIs: prefrontal cortex, DLPFC, hippocampus, and temporal cortex, which match the ROIs used for [^{18}F]-FEPPA quantification. The ICV was defined as all non-bone pixels within the skull, beginning with the first slice in which the frontal poles were visible and ending at the occipital pole. Brainstem and cerebellum were included. Total ICV for each subject was quantified by counting the voxels in a mask that was generated automatically by the Brain Extraction Tool (BET) (Smith, 2002).

DNA extraction and polymorphism genotyping

Genomic DNA was obtained from peripheral leukocytes using high salt extraction methods (Lahiri and Nurnberger, 1991). The polymorphism rs6971 was genotyped variously using a TaqMan® assay on demand C_2512465_20 (AppliedBiosystems, CA, USA). The allele T147 was linked to Vic and the allele A147 was linked FAM. PCR reactions were performed in a 96-well microtiter-plate on a GeneAmp PCR System 9700 (Applied Biosystems, CA, USA). After PCR amplification, endpoint plate read and allele calling was performed using an ABI 7900 HT (Applied Biosystems, CA, USA) and the corresponding SDS software (v2.2.2). As previously described, individuals with genotype Ala147/ Ala147 were classified as high affinity binders (HAB), Ala147/Thr147 as mixed affinity binders (MAB), and Thr147/Thr147 as low affinity binders (LAB) (Owen et al., 2012).

Statistical analysis

Statistical analysis was performed using SPSS Statistics 17.0. Demographic characteristics and PET parameters were compared between genetic groups by one-way analysis of variance (ANOVA). Repeated-measures ANOVA with multiple ROIs as within-subject variables, age and genetic group as predictor variables were used to determine the effect of age adjusting for rs6971polymorphism on mean regional [^{18}F]-FEPPA V_T across ROIs. As secondary analyses, multiple regression analyses were conducted to determine the relationship between age, genetic group, and regional [^{18}F]-FEPPA V_T on the individual ROI. Associations between regional volume ratio and age were evaluated using Pearson correlation analysis. Associations between regional [^{18}F]-FEPPA V_Ts and volume ratio were

evaluated using linear regression analysis with age entered as a covariate. The threshold for significance was set at $p < 0.05$, two-tailed for all analyses.

Results

Thirty-three individuals were included (mean ± SD age, 49.09 ± 18.6 years; 13 males and 20 females). Thirty of 33 participants were free of any medications, while 2 were taking anti-hypertensive and one was taking cholesterol-lowering medication. Visual inspection of PD-weighted MRI revealed evidence of white matter hyperintensities in the anterior and posterior horn of the lateral ventricles in one participant. The rest of the participants showed no evidence of significant vascular lesions.

Genetic analysis revealed 22 HABs (Ala147/Ala147), 11 MABs (Ala147/Thr147), and no LABs (Thr147/Thr147). All subjects are considered cognitively normal (mean MMSE score for HAB: 29.61 ± 0.608; for MAB: 29.25 ± 1.165). Due to the known influence of TSPO genotype on [^{18}F]-FEPPA in vivo binding, the examination of age relationship with [^{18}F]-FEPPA V_T in the present study was conducted with genetic group inputted as a predictor. Table 1 summarizes the demographic data, PET parameters, and regional [^{18}F]-FEPPA V_T of all subjects stratified by genetic group.

Repeated measures ANOVA revealed no significant age effect across all ROIs ($F(1,30) = 0.918$; $p = 0.346$), and a significant effect of genetic status ($F(1,30) = 8.767$; $p = 0.006$). The Greenhouse–Geisser within-subject test indicated a non-significant effect of ROI, showing that [^{18}F]-FEPPA V_T is not significantly different among brain regions ($F(1.55,46.50) = 0.680$; $p = 0.476$). There was no significant interaction between age and ROI ($F(1.55, 46.50) = 1.770$; $p = 0.188$), or between genetic group and ROI ($F(1.55, 46.50) = 3.545$; $p = 0.048$). ANOVA analyses revealed no significant interaction between age and genotype in all of the ROI examined (in the hippocampus ($F(1,29) = 0.227$, $p = 0.637$); prefrontal cortex ($F(1,29) = 2.515$, $p = 0.124$); temporal cortex ($F(1,29) = 1.763$, $p = 0.195$); DLPFC ($F(1,29) = 2.849$, $p = 0.102$)). The effect of age on [^{18}F]-FEPPA V_T remained not significant even after partial volume effect correction (PVEC) (age effect: $F(1,30) = 0.928$; $p = 0.343$; genetic effect: $F(1,30) = 9.099$; $p = 0.005$). Summary of the model and standardized beta coefficients of individual predictors in each ROI investigated are presented in Table 2. As reported in Table 2, univariate analysis of variances with both age and genetic group inputted as predictor variables did not reveal significant age effect in all the ROIs examined. The overall model with both age and genetic group as predictor variables explained a significant portion of total variation observed in regional [^{18}F]-FEPPA V_T. However, age alone did not make a significant contribution to the outcome measure in any of the examined ROIs, except in the prefrontal cortex. Figs. 1(A–D) show the relationship between age and regional [^{18}F]-FEPPA V_T in both HAB and MAB in all the ROIs. We found that among the HAB, [^{18}F]-FEPPA V_T was not associated with age, except in the prefrontal cortex areas where age was associated with an increase in [^{18}F]-FEPPA V_T (prefrontal cortex $r = 0.416$, $p = 0.054$; DLPFC $r = 0.434$, $p = 0.044$). However, the age effect in the prefrontal cortical areas was no longer signifcant after PVEC (prefrontal cortex $r = 0.320$, $p = 0.147$; DLPFC $r = 0.313$, $p = 0.156$). Among the MAB, age was not associated with [^{18}F]-FEPPA V_T in any of the regions examined before or after PVEC (all $p > 0.05$).

As expected, the Pearson correlation coefficient controlling for genetic group revealed strong negative associations between age and VOI ratio in the hippocampus ($r = -0.517$, $p = 0.002$), prefrontal cortex ($r = -0.765$, $p < 0.001$), DLPFC ($r = -0.774$, $p < 0.001$), temporal cortex ($r = -0.691$, $p < 0.001$). The correlations between age and VOI ratio for all regions remained significant after Bonferroni correction for multiple comparisons ($p = 0.05/4 = 0.01$). Linear regression analyses with age included as a covariate revealed no significant relationship between [^{18}F]-FEPPA V_T and VOI ratio in the Prefrontal cortex ($F(2,30) = 1.294$, $p = 0.289$), DLPFC ($F(2,30) = 0.957$, $p = 0.396$), temporal cortex ($F(2,30) = 0.381$, $p = 0.686$). However, a significant association in the hippocampus was found ($F(2,30) = 5.14$, $p = 0.01$).

Discussion

In the present study, we investigated the effect of age on neuroinflammation by quantifying TSPO in healthy humans using [^{18}F]-FEPPA PET. We found no significant association between age and regional [^{18}F]-FEPPA uptake. Even after considering the contribution of TSPO genetic polymorphism on [^{18}F]-FEPPA binding affinity, the relationship between [^{18}F]-FEPPA V_T and age remained not significant. As expected, age-related volume loss was found in the hippocampus, prefrontal and temporal cortex. However, we did not observe significant associations between age-related volume loss and regional [^{18}F]-FEPPA V_T in the pre-frontal and temporal cortex.

Consistent with our previous finding, we observed a considerable variation of [^{18}F]-FEPPA V_T, part of which was explained by TSPO gene polymorphism. An increasing degree of brain atrophy may affect the quantification of [^{18}F]-FEPPA in the elderly subjects. In order to correct the effect of brain atrophy, [^{18}F]-FEPPA quantification was also carried out with the PVE corrected images (Bencherif et al., 2004). Our data suggests that after correction for PVE, age was not significantly associated with an increase in [^{18}F]-FEPPA V_T in either HAB or MAB, supporting the view that age is not related to neuroinflammation in our cognitively healthy normal sample.

The current finding is consistent with a previous in-vitro study, which reported no age-related increase in TSPO density in a platelet sample of older compared to younger subjects (Marazziti et al., 1994). However, previous electron microscopy studies have noted age-related alteration in microglia morphology and function (Flanary et al., 2007; Streit et al., 2004). Our finding supports the contention that aging microglia may show features of degeneration, rather than activation. Microglial degeneration has molecular features that are distinct from activation. Degenerating microglia have dystrophic features and may have impaired cellular function, indicative of cellular senescence characterized by shorter telomere length, lower telomerase activity, and fragmented cytoplasmic processes (Flanary et al., 2007; Streit et al., 2004, 2009).

The effect of age on TSPO expression in healthy human brains in-vivo has mostly been examined using [^{11}C]-PK11195, and the results from these studies have been mixed (Cagnin et al., 2001; Debruyne et al., 2003; Kumar et al., 2012; Schuitemaker et al., 2010). The first study observed no significant relationship between age and [^{11}C]-PK11195 binding

throughout cortical and subcortical regions, except in the thalamus where a positive association was found (Cagnin et al., 2001). This finding is mostly consistent with a few other TSPO PET studies, which also did not observe age-related increased in TSPO binding in cognitively normal healthy volunteers (Debruyne et al., 2003; Yasuno et al., 2008). Recently, Kumar et al, 2012 reported significant positive correlations between age and TSPO binding using [^{11}C]-PK11195 standard uptake value (SUV) as an outcome measure (Kumar et al., 2012). However, the correlation was no longer significant when [^{11}C]-PK11195 BP_{ND} was used as an outcome measure. The authors of the study noted that the use of cerebellum as a reference region might serve as a potential methodological limitation for quantifying [^{11}C]-PK11195 binding. On the other hand, another study using the same radioligand (Schuitemaker et al., 2010) was able to detect signifi-cant increases in [^{11}C]-PK11195 binding with age using a supervised cluster analysis to extract a reference tissue input function. Nevertheless, one study using a second-generation radioligand, [^{11}C]-DAA1106 and a full kinetic analysis using arterial input function did not observe significant age effect on TSPO expression throughout the brain. Finally, a study with a newer TSPO radioligand, [^{11}C]vinpocentine reported an age-related increased in % SUV values and binding in the whole brain. However, it is possible that this radioligand might not be sufficiently sensitive to detect microglia activation in-vivo as the expected differences in binding were not found between AD patients and age-matched healthy controls (Gulyas et al., 2011).

The methodological differences between the previous and present studies are important. The majority of previous studies used [^{11}C]-PK11195 to quantify microglia activation. [^{18}F]-FEPPA binds with higher affinity to TSPO compared to PK11195 as demonstrated by a significantly lower inhibition constant (Ki) of FEPPA to PK11195. Due to its higher affinity, [^{18}F]-FEPPA may provide greater sensitivity than PK11195 as a TSPO radioligand. The higher affinity of [^{18}F]-FEPPA may overcome the low signal to noise ratio of PK11195, which has been reported in several studies (Banati et al., 2000; Groom et al., 1995; Petit-Taboue et al., 1991). A direct in vivo comparison between [^{18}F]-FEPPA and [^{11}C]-PK11195 in animal model of neuroinflammation revealed that [^{18}F]-FEPPA showed a greater contrast uptake between the lesioned and healthy area. Specifically, [^{18}F]-FEPPA displayed a similar uptake to that of [^{11}C]-PK11195 in the lesioned area, but showed lower uptake in the healthy area, demonstrating the specificity of [^{18}F]-FEPPA binding towards TSPO-enriched lesions (Hatano et al., 2010). More recently, (Ko et al., 2013) showed that [^{18}F]-FEPPA uptake was three-fold higher at the tumor site compared to the contralateral side. Further, inter-individual variability in binding affinity was observed in second-generation TSPO ligands, but not with [^{11}]-PK11195, suggesting that [^{11}]-PK11195 may bind to a different site of TSPO (Kreisl et al., 2010; Owen et al., 2010, 2011). In a recent mathematical modeling paper (Guo et al., 2012), it was suggested that the new generation of TSPO radioligands can be expected to perform better in vivo than [^{11}]-PK11195 and have superior power to detect differences in TSPO density, when the binding class information is known.

There are few factors that need to be considered regarding the use of [^{18}F]-FEPPA to examine microglia activation in the context of pathophysiological changes of aging. First, it is difficult to ascertain the sensitivity of [^{18}F]-FEPPA to detect microglia activation due to the lack of tissue studies involving immunohistochemistry and autoradiography to show a direct correlation between [^{18}F]-FEPPA accumulation and histologic stains for activated

microglia. However, co-injection of [^{18}F]-FEPPA with a pharmacological dose of a competing ligand, PK11195 in non-human primate brain resulted in a significant reduction of radioactivity, providing a convincing demonstration of [^{18}F]-FEPPA specific binding to TSPO (Hatano et al., 2010). In addition, immunohistochemical measurements of inflammatory cytokines (IL-1β, TNF-α) correlated well with the asymmetrical uptake of [^{18}F]-FEPPA (Hatano et al., 2010).

A possible explanation for the lack of relationship between neuroinflammation and age might be due to the fact that only cognitively normal individuals were included in our study. Although memory impairment is a common occurrence in aging, our healthy control samples did not show any signs of cognitive impairment as indicated by their MMSE scores. Although we acknowledge that MMSE can be used as a general test to assess cognitive performance, the use of a more comprehensive and sensitive cognitive instruments might be useful to capture small differences in cognitive status of healthy individuals with presumably intact cognitive functions.

Extreme reduction in blood flow to the brain, as in the case of cerebral ischemia/stroke is known to induce tissue damage that is associated with significant increases in TSPO expression (Martin et al., 2011; Thiel and Heiss, 2011). Age-associated reduction in blood flow is well documented (Iwata and Harano, 1986; Schultz et al., 1999; Takahashi et al., 2005). However, the correlation between age and cerebral hypoperfusion is stronger in individuals with vascular risk factors (de la Torre, 2012; Fazekas et al., 1988; Kawamura et al., 1993). In the present study, we only included healthy individuals who had no history of past cardiovascular events. Further, the majority of our study participants had no risk factors that are associated with cerebrovascular disease, such as prior cardiovascular events, atrial fibrillation, hypertension, diabetes mellitus, hypercholesterolemia, cigarette smoking and obesity (de la Torre, 2012; Wolf et al., 1991). Visual inspection of individuals' PD-weighted MRI scans revealed no evidence of significant focal cerebral and vascular lesions associated with cerebrovascular disease, except in one person where periventricular white matter hyperintensities were evident surrounding the anterior and posterior horn of lateral ventricles. The [^{18}F]-FEPPA V_T values for this individual in all ROIs investigated (both before and after partial volume error correction), were approximately 2% within the sample mean. The lack of vascular risk factors in most of our healthy participants was consistent with the preserved general cognitive function, as indicated by relatively normal cognitive test performance (MMSE scores). Therefore, we conclude that the minor ischemic changes that may occur with advancing age are unlikely to affect TSPO expression in our sample population. Indeed, the age-associated reduction in blood flow may affect the delivery of radioligand to the brain. However, previous work showed that changes in blood flow produced less than 1% change in [^{18}F]-FEPPA (V_T) (Rusjan et al., 2011). Thus, even if minor ischemic changes were present, the results of our study still do not support significant associations between age and TSPO expression in healthy aging.

It is possible that neuroinflammation represents a disease specific process that compromises cognition (Ownby, 2010). This hypothesis would be consistent with findings in patients with mild AD, where moderate memory impairment was associated with elevated TSPO ligand uptake (Cagnin et al., 2001). From the preclinical studies, increases in TSPO expression

have only been reported in animal models of disease, such as in mouse model of accelerated aging (Nomura et al., 1996) and in transgenic mice model of AD (Venneti et al., 2009), but not in wild type controls. This notion is further supported by an immunohistochemistry finding in aging rhesus monkeys using antibodies against Human Leukocytes Antigen (HLA-DR) and inducible nitric oxide synthase, markers of microglia activation, demonstrating that the density of activated microglia was significantly more elevated in cognitively impaired old monkeys, but not in the cognitively normal monkeys (Sloane et al., 1999). Few ex-vivo studies in human have reported greater density of activated microglia in the older compared to young adults (DiPatre and Gelman, 1997; Sheng et al., 1998). However, this study only included postmortem brains of individuals with no pathological evidence of neurological disease. Since neuropsychological assessments were not documented, cognitive status is unknown.

Regional decreases in brain volume have been reported to occur in normal aging (De Leon et al., 1997; Hutton et al., 2009; Salat et al., 2001; Tisserand et al., 2004). Consistent with these findings, we found age-related volume loss in all the regions examined. In a study using transgenic mouse models of AD, an elevated TSPO expression in microglia was associated with substantial neuronal loss, with the greatest TSPO expression found in areas showing the most pronounced atrophy, such as the hippocampus and entorhinal cortex (Ji et al., 2008). In our study, we did not find significant association between neuroinflammation and volume loss in any of the regions examined except in the hippocampus, where a higher volume ratio was associated with an increase in FEPPA binding. According to findings from a seminal imaging study (Cagnin et al., 2001), which examined the relationship between cortical atrophy and neuroinflammation, an increase in neuroinflammation at baseline predicts a decrease in brain volume at 12–24 months follow-up. Moreover, in clinical population such as AD (Edison et al., 2008; Papadopoulos et al., 2006), frontotemporal dementia (Cagnin et al., 2004), and Parkinson's disease (Gerhard et al., 2006; Ouchi et al., 2005), increases in TSPO ligand binding are typically localized at the sites of degenerative changes. Therefore, based on the current data in the literature, the significant positive association we found between neuroinflammation and brain volume in the hippocampus might need further confirmation in longitudinal studies. In general, the lack of relationship between [^{18}F]-FEPPA uptake and volume loss in the other regions might reflect a different spatiotemporal profile between microglia activation and cortical atrophy. Future longitudinal studies will help elucidate this relationship.

The strengths of this study are the large sample size and wide age range of study participants, the use of a second generation TSPO radioligand, [^{18}F]-FEPPA, the incorporation of genetic variants (rs6971 polymorphism) and the use of high resolution PET camera system (HRRT). Substantial brain atrophy in the older subjects might affect the assessment of [^{18}F]-FEPPA, and some regions might be more vulnerable than others. For example, the enlargement of ventricles is commonly observed with aging and might result in the contamination of PET signal; introducing partial volume errors in the neighboring brain regions. However, the use of a higher resolution PET scanner such as the HRRT should make our quantification less susceptible to these errors (Leroy et al., 2007; van Velden et al., 2009). Moreover, even after the application of a partial volume correction method (Bencherif et al., 2004), the effect of age on [^{18}F]-FEPPA V_T was not significant.

In conclusion, although advancing age is associated with regional decreases in brain volume, our study does not support that neuroinflammation, as reflected by the overexpression of TSPO, occurs during normal aging. Our findings indirectly support the utility of [^{18}F]-FEPPA in age-related disorders where neuroinflammation may be present, such as Alzheimer's disease.

Acknowledgments

This work is supported by the Scottish Grant Charitable Foundation. The authors wish to thank Armando Garcia, Winston Stableford, Min Wong, and Peter Bloomfield for their technical assistance.

References

Banati RB, Newcombe J, Gunn RN, Cagnin A, Turkheimer F, Heppner F, Price G, Wegner F, Giovannoni G, Miller DH, Perkin GD, Smith T, Hewson AK, Bydder G, Kreutzberg GW, Jones T, Cuzner ML, Myers R. The peripheral benzodiazepine binding site in the brain in multiple sclerosis: quantitative in vivo imaging of microglia as a measure of disease activity. Brain. 2000; 123(Pt 11): 2321–2337. [PubMed: 11050032]

Bencherif B, Stumpf MJ, Links JM, Frost JJ. Application of MRI-based partial-volume correction to the analysis of PET images of mu-opioid receptors using statistical parametric mapping. J Nucl Med. 2004; 45:402–408. [PubMed: 15001679]

Block ML, Hong JS. Microglia and inflammation-mediated neurodegeneration: multiple triggers with a common mechanism. Prog Neurobiol. 2005; 76:77–98. [PubMed: 16081203]

Cagnin A, Brooks DJ, Kennedy AM, Gunn RN, Myers R, Turkheimer FE, Jones T, Banati RB. In-vivo measurement of activated microglia in dementia. Lancet. 2001; 358:461–467. [PubMed: 11513911]

Cagnin A, Rossor M, Sampson EL, Mackinnon T, Banati RB. In vivo detection of microglial activation in frontotemporal dementia. Ann Neurol. 2004; 56:894–897. [PubMed: 15562429]

Chauveau F, Boutin H, Van Camp N, Dolle F, Tavitian B. Nuclear imaging of neuroinflammation: a comprehensive review of [11C]PK11195 challengers. Eur J Nucl Med Mol Imaging. 2008; 35:2304–2319. [PubMed: 18828015]

Chen MK, Guilarte TR. Translocator protein 18 kDa (TSPO): molecular sensor of brain injury and repair. Pharmacol Ther. 2008; 118:1–17. [PubMed: 18374421]

Damani MR, Zhao L, Fontainhas AM, Amaral J, Fariss RN, Wong WT. Age-related alterations in the dynamic behavior of microglia. Aging Cell. 2011; 10:263–276. [PubMed: 21108733]

de la Torre JC. Cardiovascular risk factors promote brain hypoperfusion leading to cognitive decline and dementia. Cardiovasc Psychiatry Neurol. 2012; 2012:367516. [PubMed: 23243502]

De Leon MJ, George AE, Golomb J, Tarshish C, Convit A, Kluger A, De Santi S, McRae T, Ferris SH, Reisberg B, Ince C, Rusinek H, Bobinski M, Quinn B, Miller DC, Wisniewski HM. Frequency of hippocampal formation atrophy in normal aging and Alzheimer's disease. Neurobiol Aging. 1997; 18:1–11. [PubMed: 8983027]

Debruyne JC, Versijpt J, Van Laere KJ, De Vos F, Keppens J, Strijckmans K, Achten E, Slegers G, Dierckx RA, Korf J, De Reuck JL. PET visualization of microglia in multiple sclerosis patients using [11C]PK11195. Eur J Neurol. 2003; 10:257–264. [PubMed: 12752399]

DiPatre PL, Gelman BB. Microglial cell activation in aging and Alzheimer disease: partial linkage with neurofibrillary tangle burden in the hippocampus. J Neuropathol Exp Neurol. 1997; 56:143–149. [PubMed: 9034367]

Edison P, Archer HA, Gerhard A, Hinz R, Pavese N, Turkheimer FE, Hammers A, Tai YF, Fox N, Kennedy A, Rossor M, Brooks DJ. Microglia, amyloid, and cognition in Alzheimer's disease: an [11C](R)PK11195-PET and [11C]PIB-PET study. Neurobiol Dis. 2008; 32:412–419. [PubMed: 18786637]

Fazekas F, Niederkorn K, Schmidt R, Offenbacher H, Horner S, Bertha G, Lechner H. White matter signal abnormalities in normal individuals: correlation with carotid ultrasonography, cerebral

blood flow measurements, and cerebrovascular risk factors. Stroke. 1988; 19:1285–1288. [PubMed: 3051534]

Flanary BE, Sammons NW, Nguyen C, Walker D, Streit WJ. Evidence that aging and amyloid promote microglial cell senescence. Rejuvenation Res. 2007; 10:61–74. [PubMed: 17378753]

Fujita M, Imaizumi M, Zoghbi SS, Fujimura Y, Farris AG, Suhara T, Hong J, Pike VW, Innis RB. Kinetic analysis in healthy humans of a novel positron emission tomography radioligand to image the peripheral benzodiazepine receptor, a potential biomarker for inflammation. Neuroimage. 2008; 40:43–52. [PubMed: 18093844]

Gehrmann J, Matsumoto Y, Kreutzberg GW. Microglia: intrinsic immuneffector cell of the brain. Brain Res Brain Res Rev. 1995; 20:269–287. [PubMed: 7550361]

Gerhard A, Neumaier B, Elitok E, Glatting G, Ries V, Tomczak R, Ludolph AC, Reske SN. In vivo imaging of activated microglia using [11C]PK11195 and positron emission tomography in patients after ischemic stroke. Neuroreport. 2000; 11:2957–2960. [PubMed: 11006973]

Gerhard A, Pavese N, Hotton G, Turkheimer F, Es M, Hammers A, Eggert K, Oertel W, Banati RB, Brooks DJ. In vivo imaging of microglial activation with [11C](R)-PK11195 PET in idiopathic Parkinson's disease. Neurobiol Dis. 2006; 21:404–412. [PubMed: 16182554]

Godbout JP, Johnson RW. Age and neuroinflammation: a lifetime of psychoneuroimmune consequences. Neurol Clin. 2006; 24:521–538. [PubMed: 16877122]

Groom GN, Junck L, Foster NL, Frey KA, Kuhl DE. PET of peripheral benzodiazepine binding sites in the microgliosis of Alzheimer's disease. J Nucl Med. 1995; 36:2207–2210. [PubMed: 8523106]

Gulyas B, Vas A, Toth M, Takano A, Varrone A, Cselenyi Z, Schain M, Mattsson P, Halldin C. Age and disease related changes in the translocator protein (TSPO) system in the human brain: positron emission tomography measurements with [11C]vinpocetine. Neuroimage. 2011; 56:1111–1121. [PubMed: 21320609]

Guo Q, Owen DR, Rabiner EA, Turkheimer FE, Gunn RN. Identifying improved TSPO PET imaging probes through biomathematics: the impact of multiple TSPO binding sites in vivo. Neuroimage. 2012; 60:902–910. [PubMed: 22251896]

Hatano K, Yamada T, et al. Correlation between FEPPA uptake and microglia activation in 6-OHDA injured rat brain. Neuroimage. 2010; 52(Suppl 1):S138–S138.

Henry CJ, Huang Y, Wynne AM, Godbout JP. Peripheral lipopolysaccharide (LPS) challenge promotes microglial hyperactivity in aged mice that is associated with exaggerated induction of both pro-inflammatory IL-1beta and anti-inflammatory IL-10 cytokines. Brain Behav Immun. 2009; 23:309–317. [PubMed: 18814846]

Hutton C, Draganski B, Ashburner J, Weiskopf N. A comparison between voxel-based cortical thickness and voxel-based morphometry in normal aging. Neuroimage. 2009; 48:371–380. [PubMed: 19559801]

Iwata K, Harano H. Regional cerebral blood flow changes in aging. Acta Radiol Suppl. 1986; 369:440–443. [PubMed: 2980521]

Jack CR Jr, Petersen RC, Xu YC, Waring SC, O'Brien PC, Tangalos EG, Smith GE, Ivnik RJ, Kokmen E. Medial temporal atrophy on MRI in normal aging and very mild Alzheimer's disease. Neurology. 1997; 49:786–794. [PubMed: 9305341]

Jernigan TL, Archibald SL, Fennema-Notestine C, Gamst AC, Stout JC, Bonner J, Hesselink JR. Effects of age on tissues and regions of the cerebrum and cerebellum. Neurobiol Aging. 2001; 22:581–594. [PubMed: 11445259]

Ji B, Maeda J, Sawada M, Ono M, Okauchi T, Inaji M, Zhang MR, Suzuki K, Ando K, Staufenbiel M, Trojanowski JQ, Lee VM, Higuchi M, Suhara T. Imaging of peripheral benzodiazepine receptor expression as biomarkers of detrimental versus beneficial glial responses in mouse models of Alzheimer's and other CNS pathologies. J Neurosci. 2008; 28:12255–12267. [PubMed: 19020019]

Kawamura J, Terayama Y, Takashima S, Obara K, Pavol MA, Meyer JS, Mortel KF, Weathers S. Leuko-araiosis and cerebral perfusion in normal aging. Exp Aging Res. 1993; 19:225–240. [PubMed: 8223824]

Ko JH, Koshimori Y, Mizrahi R, Rusjan P, Wilson AA, Lang AE, Houle S, Strafella AP. Voxel-based imaging of translocator protein 18 kDa (TSPO) in high-resolution PET. J Cereb Blood Flow Metab. 2013; 33:348–350. [PubMed: 23281426]

Kreisl WC, Fujita M, Fujimura Y, Kimura N, Jenko KJ, Kannan P, Hong J, Morse CL, Zoghbi SS, Gladding RL, Jacobson S, Oh U, Pike VW, Innis RB. Comparison of [(11)C]-(R)-PK 11195 and [(11)C]PBR28, two radioligands for translocator protein (18 kDa) in human and monkey: implications for positron emission tomographic imaging of this inflammation biomarker. Neuroimage. 2010; 49:2924–2932. [PubMed: 19948230]

Kreisl WC, Jenko KJ, Hines CS, Hyoung Lyoo C, Corona W, Morse CL, Zoghbi SS, Hyde T, Kleinman JE, Pike VW, McMahon FJ, Innis RB. A genetic polymorphism for translocator protein 18 kDa affects both in vitro and in vivo radioligand binding in human brain to this putative biomarker of neuroinflammation. J Cereb Blood Flow Metab. 2013; 33:53–58. [PubMed: 22968319]

Kumar A, Muzik O, Shandal V, Chugani D, Chakraborty P, Chugani HT. Evaluation of age-related changes in translocator protein (TSPO) in human brain using (11)C-[R]-PK11195 PET. J Neuroinflammation. 2012; 9:232. [PubMed: 23035793]

Lahiri DK, Nurnberger JI Jr. A rapid non-enzymatic method for the preparation of HMW DNA from blood for RFLP studies. Nucleic Acids Res. 1991; 19:5444. [PubMed: 1681511]

Lekander M, Von Essen J, Schultzberg M, Andreasson AN, Garlind A, Hansson LO, Nilsson LG. Cytokines and memory across the mature life span of women. Scand J Psychol. 2011; 52:229–235. [PubMed: 21332483]

Leroy C, Comtat C, Trebossen R, Syrota A, Martinot JL, Ribeiro MJ. Assessment of 11C-PE2I binding to the neuronal dopamine transporter in humans with the high-spatial-resolution PET scanner HRRT. J Nucl Med. 2007; 48:538–546. [PubMed: 17401089]

Maldjian JA, Laurienti PJ, Kraft RA, Burdette JH. An automated method for neuroanatomic and cytoarchitectonic atlas-based interrogation of fMRI data sets. Neuroimage. 2003; 19:1233–1239. [PubMed: 12880848]

Marazziti D, Pancioli-Guadagnucci ML, Rotondo A, Giannaccini G, Martini C, Lucacchini A, Cassano GB. Age-related changes in peripheral benzodiazepine receptors of human platelets. J Psychiatry Neurosci. 1994; 19:136–139. [PubMed: 8204565]

Martin A, Boisgard R, Kassiou M, Dolle F, Tavitian B. Reduced PBR/TSPO expression after minocycline treatment in a rat model of focal cerebral ischemia: a PET study using [(18)F]DPA-714. Mol Imaging Biol. 2011; 13:10–15. [PubMed: 20383592]

Miller KR, Streit WJ. The effects of aging, injury and disease on microglial function: a case for cellular senescence. Neuron Glia Biol. 2007; 3:245–253. [PubMed: 18634615]

Mizrahi R, Rusjan PM, Kennedy J, Pollock B, Mulsant B, Suridjan I, De Luca V, Wilson AA, Houle S. Translocator protein (18 kDa) polymorphism (rs6971) explains in-vivo brain binding affinity of the PET radioligand [(18)F]-FEPPA. J Cereb Blood Flow Metab. 2012; 32:968–972. [PubMed: 22472607]

Muller-Gartner HW, Links JM, Prince JL, Bryan RN, McVeigh E, Leal JP, Davatzikos C, Frost JJ. Measurement of radiotracer concentration in brain gray matter using positron emission tomography: MRI-based correction for partial volume effects. J Cereb Blood Flow Metab. 1992; 12:571–583. [PubMed: 1618936]

Njie EG, Boelen E, Stassen FR, Steinbusch HW, Borchelt DR, Streit WJ. Ex vivo cultures of microglia from young and aged rodent brain reveal age-related changes in microglial function. Neurobiol Aging. 2012; 33(195):e191–112.

Nomura Y, Yamanaka Y, Kitamura Y, Arima T, Ohnuki T, Oomura Y, Sasaki K, Nagashima K, Ihara Y. Senescence-accelerated mouse. Neurochemical studies on aging. Ann N Y Acad Sci. 1996; 786:410–418. [PubMed: 8687038]

Okello A, Edison P, Archer HA, Turkheimer FE, Kennedy J, Bullock R, Walker Z, Kennedy A, Fox N, Rossor M, Brooks DJ. Microglial activation and amyloid deposition in mild cognitive impairment: a PET study. Neurology. 2009; 72:56–62. [PubMed: 19122031]

Ouchi Y, Yoshikawa E, Sekine Y, Futatsubashi M, Kanno T, Ogusu T, Torizuka T. Microglial activation and dopamine terminal loss in early Parkinson's disease. Ann Neurol. 2005; 57:168–175. [PubMed: 15668962]

Owen DR, Gunn RN, Rabiner EA, Bennacef I, Fujita M, Kreisl WC, Innis RB, Pike VW, Reynolds R, Matthews PM, Parker CA. Mixed-affnity binding in humans with 18-kDa translocator protein ligands. J Nucl Med. 2011; 52:24–32. [PubMed: 21149489]

Owen DR, Howell OW, Tang SP, Wells LA, Bennacef I, Bergstrom M, Gunn RN, Rabiner EA, Wilkins MR, Reynolds R, Matthews PM, Parker CA. Two binding sites for [3H]PBR28 in human brain: implications for TSPO PET imaging of neuroinflammation. J Cereb Blood Flow Metab. 2010; 30:1608–1618. [PubMed: 20424634]

Owen DR, Yeo AJ, Gunn RN, Song K, Wadsworth G, Lewis A, Rhodes C, Pulford DJ, Bennacef I, Parker CA, StJean PL, Cardon LR, Mooser VE, Matthews PM, Rabiner EA, Rubio JP. An 18-kDa translocator protein (TSPO) polymorphism explains differences in binding affinity of the PET radioligand PBR28. J Cereb Blood Flow Metab. 2012; 32:1–5. [PubMed: 22008728]

Ownby RL. Neuroinflammation and cognitive aging. Curr Psychiatry Rep. 2010; 12:39–45. [PubMed: 20425309]

Papadopoulos V, Lecanu L, Brown RC, Han Z, Yao ZX. Peripheral-type benzo-diazepine receptor in neurosteroid biosynthesis, neuropathology and neurological disorders. Neuroscience. 2006; 138:749–756. [PubMed: 16338086]

Pappata S, Levasseur M, Gunn RN, Myers R, Crouzel C, Syrota A, Jones T, Kreutzberg GW, Banati RB. Thalamic microglial activation in ischemic stroke detected in vivo by PET and [11C]PK1195. Neurology. 2000; 55:1052–1054. [PubMed: 11061271]

Peters A, Josephson K, Vincent SL. Effects of aging on the neuroglial cells and pericytes within area 17 of the rhesus monkey cerebral cortex. Anat Rec. 1991; 229:384–398. [PubMed: 2024779]

Petit-Taboue MC, Baron JC, Barre L, Travere JM, Speckel D, Camsonne R, MacKenzie ET. Brain kinetics and specific binding of [11C]PK 11195 to omega 3 sites in baboons: positron emission tomography study. Eur J Pharmacol. 1991; 200:347–351. [PubMed: 1782994]

Rajkowska G, Goldman-Rakic PS. Cytoarchitectonic definition of prefrontal areas in the normal human cortex: I. Remapping of areas 9 and 46 using quantitative criteria. Cereb Cortex. 1995a; 5:307–322. [PubMed: 7580124]

Rajkowska G, Goldman-Rakic PS. Cytoarchitectonic definition of prefrontal areas in the normal human cortex: II. Variability in locations of areas 9 and 46 and relationship to the Talairach Coordinate System. Cereb Cortex. 1995b; 5:323–337. [PubMed: 7580125]

Raz N, Gunning FM, Head D, Dupuis JH, McQuain J, Briggs SD, Loken WJ, Thornton AE, Acker JD. Selective aging of the human cerebral cortex observed in vivo: differential vulnerability of the prefrontal gray matter. Cereb Cortex. 1997; 7:268–282. [PubMed: 9143446]

Rusjan P, Mamo D, Ginovart N, Hussey D, Vitcu I, Yasuno F, Tetsuya S, Houle S, Kapur S. An automated method for the extraction of regional data from PET images. Psychiatry Res. 2006; 147:79–89. [PubMed: 16797168]

Rusjan PM, Wilson AA, Bloomfield PM, Vitcu I, Meyer JH, Houle S, Mizrahi R. Quantitation of translocator protein binding in human brain with the novel radioligand [18F]-FEPPA and positron emission tomography. J Cereb Blood Flow Metab. 2011; 31:1807–1816. [PubMed: 21522163]

Salat DH, Kaye JA, Janowsky JS. Prefrontal gray and white matter volumes in healthy aging and Alzheimer disease. Arch Neurol. 1999; 56:338–344. [PubMed: 10190825]

Salat DH, Kaye JA, Janowsky JS. Selective preservation and degeneration within the prefrontal cortex in aging and Alzheimer disease. Arch Neurol. 2001; 58:1403–1408. [PubMed: 11559311]

Schuitemaker A, van der Doef TF, Boellaard R, van der Flier WM, Yaqub M, Windhorst AD, Barkhof F, Jonker C, Kloet RW, Lammertsma AA, Scheltens P, van Berckel BN. Microglial activation in healthy aging. Neurobiol Aging. 2010; 33:1067–1072. [PubMed: 21051106]

Schultz SK, O'Leary DS, Boles Ponto LL, Watkins GL, Hichwa RD, Andreasen NC. Age-related changes in regional cerebral blood flow among young to mid-life adults. Neuroreport. 1999; 10:2493–2496. [PubMed: 10574358]

Sheffield LG, Berman NE. Microglial expression of MHC class II increases in normal aging of nonhuman primates. Neurobiol Aging. 1998; 19:47–55. [PubMed: 9562503]

Sheng JG, Mrak RE, Griffin WS. Enlarged and phagocytic, but not primed, interleukin-1 alpha-immunoreactive microglia increase with age in normal human brain. Acta Neuropathol. 1998; 95:229–234. [PubMed: 9542587]

Sierra A, Gottfried-Blackmore AC, McEwen BS, Bulloch K. Microglia derived from aging mice exhibit an altered inflammatory profile. Glia. 2007; 55:412–424. [PubMed: 17203473]

Sloane JA, Hollander W, Moss MB, Rosene DL, Abraham CR. Increased microglial activation and protein nitration in white matter of the aging monkey. Neurobiol Aging. 1999; 20:395–405. [PubMed: 10604432]

Smith SM. Fast robust automated brain extraction. Hum Brain Mapp. 2002; 17:143–155. [PubMed: 12391568]

Streit WJ, Braak H, Xue QS, Bechmann I. Dystrophic (senescent) rather than activated microglial cells are associated with tau pathology and likely precede neurodegeneration in Alzheimer's disease. Acta Neuropathol. 2009; 118:475–485. [PubMed: 19513731]

Streit WJ, Sammons NW, Kuhns AJ, Sparks DL. Dystrophic microglia in the aging human brain. Glia. 2004; 45:208–212. [PubMed: 14730714]

Studholme C, Hill DL, Hawkes DJ. Automated three-dimensional registration of magnetic resonance and positron emission tomography brain images by multi-resolution optimization of voxel similarity measures. Med Phys. 1997; 24:25–35. [PubMed: 9029539]

Takahashi K, Yamaguchi S, Kobayashi S, Yamamoto Y. Effects of aging on regional cerebral blood flow assessed by using technetium Tc 99 m hexamethylpropyleneamine oxime single-photon emission tomography with 3D stereotactic surface projection analysis. AJNR Am J Neuroradiol. 2005; 26:2005–2009. [PubMed: 16155150]

Thiel A, Heiss WD. Imaging of microglia activation in stroke. Stroke. 2011; 42:507–512. [PubMed: 21164114]

Tisserand DJ, Pruessner JC, Sanz Arigita EJ, van Boxtel MP, Evans AC, Jolles J, Uylings HB. Regional frontal cortical volumes decrease differentially in aging: an MRI study to compare volumetric approaches and voxel-based morphometry. Neuroimage. 2002; 17:657–669. [PubMed: 12377141]

Tisserand DJ, van Boxtel MP, Pruessner JC, Hofman P, Evans AC, Jolles J. A voxel-based morphometric study to determine individual differences in gray matter density associated with age and cognitive change over time. Cereb Cortex. 2004; 14:966–973. [PubMed: 15115735]

van Velden FH, Kloet RW, van Berckel BN, Buijs FL, Luurtsema G, Lammertsma AA, Boellaard R. HRRT versus HR + human brain PET studies: an interscanner test-retest study. J Nucl Med. 2009; 50:693–702. [PubMed: 19372482]

Vaughan DW, Peters A. Neuroglial cells in the cerebral cortex of rats from young adulthood to old age: an electron microscope study. J Neurocytol. 1974; 3:405–429. [PubMed: 4373545]

Venneti S, Lopresti BJ, Wang G, Hamilton RL, Mathis CA, Klunk WE, Apte UM, Wiley CA. PK11195 labels activated microglia in Alzheimer's disease and in vivo in a mouse model using PET. Neurobiol Aging. 2009; 30:1217–1226. [PubMed: 18178291]

Wiley CA, Lopresti BJ, Venneti S, Price J, Klunk WE, DeKosky ST, Mathis CA. Carbon 11-labeled Pittsburgh Compound B and carbon 11-labeled (R)-PK11195 positron emission tomographic imaging in Alzheimer disease. Arch Neurol. 2009; 66:60–67. [PubMed: 19139300]

Wilson AA, Garcia A, Parkes J, McCormick P, Stephenson KA, Houle S, Vasdev N. Radiosynthesis and initial evaluation of [18F]-FEPPA for PET imaging of peripheral benzodiazepine receptors. Nucl Med Biol. 2008; 35:305–314. [PubMed: 18355686]

Wolf PA, D'Agostino RB, Belanger AJ, Kannel WB. Probability of stroke: a risk profile from the Framingham Study. Stroke. 1991; 22:312–318. [PubMed: 2003301]

Yasuno F, Ota M, Kosaka J, Ito H, Higuchi M, Doronbekov TK, Nozaki S, Fujimura Y, Koeda M, Asada T, Suhara T. Increased binding of peripheral benzodiazepine receptor in Alzheimer's disease measured by positron emission tomography with [11C]DAA1106. Biol Psychiatry. 2008; 64:835–841. [PubMed: 18514164]

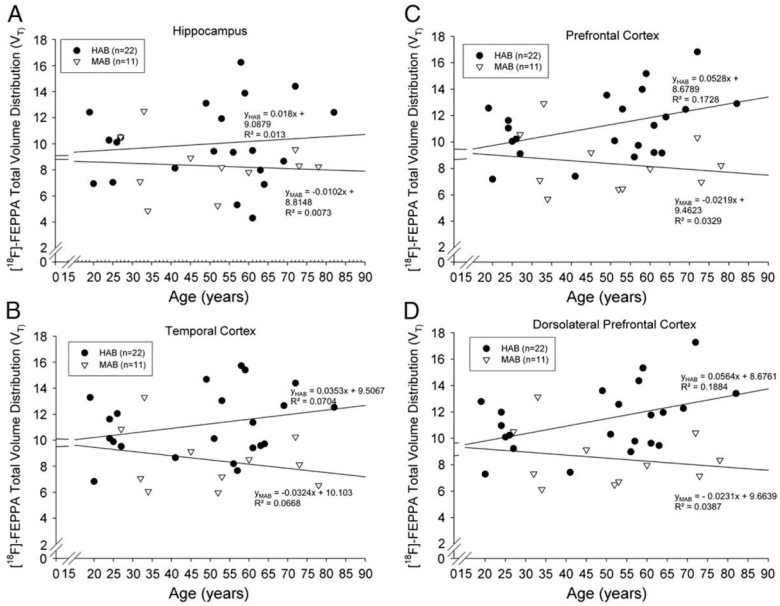

Fig. 1.

(A–D). Linear regression showing the relationship between age and [^{18}F]-FEPPA total volume distribution (V_T) in the hippocampus, temporal cortex, prefrontal cortex, and dorsolateral prefrontal cortex (not PVEC). Solid circles represent the high affinity binders (HAB); open triangles represent the mixed affinity binders (MAB).

Table 1

Demographic, PET parameters, and regional [^{18}F]-FEPPA V_T stratified by genetic groups.

Descriptive		**High affinity binders (HAB) (n = 22)**		**Mixed-affinity binders (MAB) (n = 11)**		**ANOVA between-subject**	
		mean	**sd**	**mean**	**sd**	**F(1,31)**	**p**
Age (years)		48.23	19.11	50.82	18.24	0.14	0.71
Gender	Male	10		3			
	Female	12		8			
Injected parameters	Amount injected (MBq)	178.80	14.17	176.43	9.75	0.25	0.62
	Specific activity (GBq/μmol)	154.34	127.55	116.02	120.79	0.68	0.41
	Mass injected (μg)	0.98	0.91	0.95	0.63	0.01	0.94
Regional [^{18}F]-FEPPA V_T	Hippocampus	9.96	3.02	8.30	2.17	2.62	0.12
	Temporal Ctx	11.21	2.54	8.46	2.29	9.17	0.00
	Prefrontal Ctx	11.22	2.43	8.35	2.20	10.91	0.00
	Dorsolateral Ctx	11.40	2.48	8.49	2.15	10.95	0.00

Table 2

Multiple Regression Analyses showing relationships between predictors (age and genetic) and regional [^{18}F]-FEPPA Total Volume Distribution (V_T).

		Model		Age effect		Genetic effect	
Regions of interest (ROI)	**Adjusted R square**	**F**	**p**	**Standardized coefficient beta**	**Sig**	**Standardized coefficient beta**	**Sig**
Hippocampus	0.02	1.3.4	0.28	0.06	0.73	−0.28	0.12
Temporal Ctx	0.19	4.69	0.02	0.10	0.54	−0.48	0.01
Prefrontal Ctx	0.26	6.53	0.00	0.21	0.18	−3.43	0.00
Dorsolateral Prefrontal Ctx	0.26	6.72	0.00	0.22	0.16	−0.53	0.00